- In-vivo single-cell fluorescence and the size-scaling
- of phytoplankton chlorophyll content 2
- Eva Álvarez#\* 3
- 4 Enrique Nogueira
- 5 Ángel López-Urrutia

**AEM Accepted Manuscript Posted Online 23 January 2017** Appl. Environ. Microbiol. doi:10.1128/AEM.03317-16

Copyright © 2017 American Society for Microbiology. All Rights Reserved.

- 6
- 7 Instituto Español de Oceanografía. Centro Oceanográfico de Gijón, Asturias, Spain.
- 8 Running title: The size-scaling of phytoplankton chlorophyll content
- 9
- #Address correspondence to Eva Álvarez, eva.alvarez.suarez@gmail.com 10
- 11 \*Present address: Alfred-Wegener-Institut, Helmholtz-Zentrum für Polar-und
- 12 Meeresforschung, Bremerhaven, Germany.
- 13
- 14

Downloaded from http://aem.asm.org/ on February 9, 2017 by UNIV OF CALIF SAN DIEGO

### **Abstract**

15

16

17

18

19

20

21

22

23

24

25

26

27

28

29

30

31

32

33

34

35

36

37

38

39

In unicellular phytoplankton, the size scaling exponent of chlorophyll content per cell decreases with increasing light limitation. Empirical studies have explored this allometry combining data from several species using average values of pigment content and cell size for each species. The resulting allometry, includes thus phylogenetic and size scaling effects. The possibility of measuring single-cell fluorescence with imaging-in-flow cytometry devices allows the study of the size scaling of chlorophyll content at both the inter and intra-specific levels. In this work, the changing allometry of chlorophyll content was estimated for the first time for single phytoplankton populations using data from a series of incubations with monocultures exposed to different light levels. Inter-specifically, our experiments confirm previous modelling and experimental results of increasing size scaling exponents with increasing irradiance. A similar pattern was observed intra-specifically but with a larger variability in size scaling exponents. Our results show that size-based processes and geometrical approaches explain variations in chlorophyll content. We also show that the single cell fluorescence measurements provided by imaging-in-flow devices can be applied to field samples to understand the changes in the size dependence of chlorophyll content in response to environmental variables affecting primary production.

Downloaded from http://aem.asm.org/ on February 9, 2017 by UNIV OF CALIF SAN DIEGO

**Importance** 

The chlorophyll concentrations in phytoplankton register physiological adjustments in cellular pigmentation arising mainly from changes in light conditions. The extent of these adjustments is constrained by the size of the phytoplankton cells, even within single populations. Hence, variations in community chlorophyll derived from photoacclimation are also dependent on the phytoplankton size distribution.

### Introduction

The growth rate of phytoplankton cells in the oceans is limited by resource availability,
such as light and nutrients (1). In order to maximize the efficiency of resource acquisition in a
variable environment, cell physiology adjusts through a suite of acclimation processes.
Photoacclimation refers to the phenotypic adjustments of the cells in response to variation in
irradiance levels and it is typically reflected in a graded reduction in the photosynthetic
pigment content with increasing irradiance (2). The mechanistic basis for the pigment
content-irradiance relationship is well known (3, 4) and leads to altered cellular pigment
composition.
Because all phototrophic plankton contain chlorophyll a (Chl-a) as light harvesting
pigment, it is arguably the best known and most widely used proxy for autotrophic biomass
(5). However, changes in the ratio of Chl-a to carbon biomass indicate an adjustment of
cellular pigment levels to match the demands for photosynthesis (6) and the concentration of
Chl-a is thus a biased estimator of phytoplankton biomass expressed in organic carbon terms
(1). Instead, the intra-cellular Chl- $a$ concentration can give a vision of the physiological status
of the cells which can be translated to the community level.
Phytoplankton cells adjust the Chl-a to carbon biomass ratio (Chl-a:C) in response to an
imbalance between the rate of light absorption and the energy demands for photosynthesis
and biosynthesis (7). Hence, Chl-a:C does not only varies in response to changes in light, but
also in growth rate (6). A reduction in growth rate increases Chl-a:C, and growth rate
explained 39% of Chl-a:C variability (8). Nutrient availability also influences Chl-a:C (9)

Downloaded from http://aem.asm.org/ on February 9, 2017 by UNIV OF CALIF SAN DIEGO

Light utilization traits, such as pigment content, are thought to be explained in part by cell size (12, 13). When resources are limiting, the cell surface area to volume ratio imposes

since chlorophyll synthesis is a function of the nitrogen status (10). Regarding taxonomy, the

average Chl-a:C varies for different taxonomical groups of phytoplankton (11).

66

67

68

69

70

71

72

73

74

75

76

77

78

79

80

81

82

83

84

85

86

87

88

89

fundamental constrains on the rates of resource acquisition (14). The 'package' effect is defined as a reduction in the absorption of pigmented particles within a cell relative to the absorption of the same pigments in solution. The explanation is purely geometrical: as cell volume increases internal optical pathlengths increase, limiting the absorptive efficiency of Chl-a molecules through self-shading, and, as a result, larger cells tend to have relatively lower intracellular concentrations of Chl-a than smaller cells to limit shading effects due to the packaging of pigments (13, 15). This translates into a size dependence of Chl-a content that has been reported in laboratory experiments (16) and field studies (17, 18). Additionally, cell size can vary with irradiance and the phase of cellular cycle (19), hence, changes in pigment content can be due to changes in size and not only to photoacclimation processes. It is, then, crucial considering the cellular size when dealing with changes in the elemental composition of phytoplankton.

The size dependence of photoacclimation response results in different allometric exponents in the size-scaling of Chl-a content with changing irradiance (15). The photosynthetic response to varying irradiance was described theoretically as a function of cell size (V), considering an optimal light-harvesting strategy (15), and calculating the intracellular pigment concentration required to maximize photosynthesis for a given cell size and a given irradiance. The model predicted that the optimal chlorophyll concentration is proportional to V<sup>34</sup> under light saturation and to V<sup>23</sup> under light limitation. The prediction of different allometric exponents was tested using data from different species cultured in the lab (20), which does not permit exclusion of the variability due to taxonomical composition. The calculation of allometric exponents on a single cell basis would allow testing this prediction in single populations. Hence, the same species evaluated along its whole size range would allow to observe the size-dependence of chlorophyll content without the effect of inter-specific variability.

91

92

93

94

95

96

97

98

99

100

101

102

103

104

105

106

107

108

109

110

111

112

113

The cell-level perspective provided by flow cytometry and the capacity to measure large numbers of cells has been used extensively by biological oceanographers to define the distributions and dynamics of marine pico-phytoplankton. Flow cytometry techniques allowed the quantification of optical properties, such as Chl-a auto-fluorescence, on individual cells (21). Chl-a absorbs energy from light and releases it through several phenomena, being one of them the emission of fluorescence in the red portion of the spectrum, thus, the fluorescence of Chl-a reflects the endogenous concentration of this pigment. This is the rationale for the estimation of Chl-a in situ by means of fluorometers (22) or for the measurement on discrete samples by means of fluorometric methods (23). Chl-a fluorescence intensity quantified by flow cytometry has been shown to scale with cellular Chl-a levels in nano-phytoplankton (24), but the relationships reported are not constant for all taxa due to differences in intracellular pigment structure or, even for the same taxa, due to differences in growth conditions. Hence, none of these studies provide a taxon-independent conversion from fluorescence to Chl-a that can be applied to natural samples.

In addition, traditional flow cytometers have a limited capacity to analyze large-sized phytoplankton (>5 µm). There are no measurements of fluorescence on a single cell basis for micro-plankton, a compartment where a significant proportion of the autotrophic activity takes place. The Flow Cytometer And Microscope (FlowCAM) is an automated technique for plankton enumeration that combines flow cytometry and microscopy (25). Although the FlowCAM is not a flow cytometer per se, it contains the needed elements to measure the fluorescent response of single cells: a source of light, a fluidics system in which the cells are embedded and a detection sensor. When a suspension of phototrophic cells runs through the fluidics system, the detected fluorescence signals trigger the digital camera to obtain images that allows counting and sizing the cells in the sample. However, the fluorescence signals

115

116

117

118

119

120

121

122

123

124

125

126

127

128

measured by FlowCAM have not been yet interpreted further than determining cell viability (26).

Here, we present a reliable methodology for the estimation of the content of Chl-a on single cells that allows the exploration of the changes in the size scaling of Chl-a content when cells are exposed to light limitation and that can be applied to field studies. Seven species of marine phytoplankton where grown over a range of irradiances and non-limiting nutrient conditions, and their content in pigments and fluorescence monitored to describe the relationship between the FlowCAM measured fluorescence per cell and the content of Chl-a per cell. With those cultured species we explored the changes in the inter-specific and intraspecific size scaling of Chl-a content. Finally, the size scaling of Chl-a content in field samples was explored and related to the irradiance levels in the water column. Our results showed that the allometry of the content of Chl-a changed with light intensity. This physiological responses and the size-dependence of Chl-a content can be monitored in field samples thanks to the measurement of Chl-a content on a single cell basis with imaging-inflow devices.

Downloaded from http://aem.asm.org/ on February 9, 2017 by UNIV OF CALIF SAN DIEGO

## **Materials and Methods**

### Phytoplankton cultures and growth conditions

We performed a series of incubation experiments to induce photoacclimation in cultured
phytoplankton, exposing mono-specific suspensions of cells to different light intensities in
order to obtain a gradient of intracellular Chl-a concentration. Seven species were used:
Isochrysis galbana, Emiliania huxleyi, Rhodomonas salina, Prorocentrum micans,
Karlodinium veneficum (micrum), Alexandrium tamarense and Protoceratium reticulatum.
The inocula were maintained in exponential growth in F2 media at 15 °C in a culture chamber
with photoperiod 12L:12D and low light conditions. With those initial cultures we conducted
12 experiments (Table I).
Each experiment took place in a linear incubator illuminated at one end by a spot light.
The incubator was divided into compartments along its axis by means of transverse partitions
consisting on a double layer of nylon mesh. The initial culture was divided in 50 mL cellstack
culture chambers (Corning), and the chambers placed into the compartments of the incubator.
Total irradiance (photosynthetically active radiation, PAR) in each compartment was
measured with a LICOR radiometer (Biospherical). The irradiances varied slightly between
experiments but in any one experiment light levels ranged between 37 and 1838 $\mu mol\ photons$
$\mbox{m}^{\text{-}2}~\mbox{s}^{\text{-}1}$ of PAR. Running water through the incubator maintained the temperature stable at
$15.5 \pm 0.5$ °C. Incubations were kept with constant photoperiod during 6 days in most cases to
allow photoacclimation. Samples for analysis were taken always at 9:00AM, two hours after
the light was activated. The culture chambers were shaken manually twice a day.
Experiments 1 to 4 were run by duplicate, in parallel incubator lines; samples for
microscopy counts, estimation of Chl a concentration and in vivo FlowCAM analysis were

Downloaded from http://aem.asm.org/ on February 9, 2017 by UNIV OF CALIF SAN DIEGO

taken on the last day of each incubation experiment. Experiments 5 to 12 were run in a single

154

155

156

157

158

159

160

161

162

163

164

165

166

167

168

169

170

171

172

173

174

175

176

177

178

incubator line; samples were taken on the first and last days of each incubation experiment, and additionally in the mid-term of experiments 8 and 11 (Table I).

Microscopy counts were carried out placing 1 mL of sample in a Sedgwick-Rafter counting cell slide under a NIKON inverted microscope. For the analysis of Chl-a concentration, 10mL of each sample were filtered onto Whatman GF/F filters, frozen at -18 °C during 24h and extracted in 3 mL of acetone during 24h. Chl-a a concentration was determined using a spectrofluorometer (Perkin Elmer LB-50s) with excitation set at 488 nm and emission at 663.5 nm. The signal of the spectrofluorometer was calibrated against Chl-a solutions of known concentration. The concentration of extracted Chl-a was divided by the number of cells to obtain the Chl-a per cell value, and by the total cellular volume to obtain the average intracellular Chl-a concentration.

In vivo FlowCAM analysis provided measurements of cell concentration and of single cell fluorescence and size. Excitation illumination consisted of a blue laser fan of  $488 \pm 0.04$ nm, and fluorescence was measured as the emitted light passing a 650 nm long-pass filter reaching a photomultiplier tube (PMT 1). When the fluorescent light reaches the PMT generates a voltage pulse that is described numerically by three parameters: the maximum value reached by the pulse, known as height or peak, the number of consecutive measurements that exceeded the threshold value, called width, and the integrated area under the pulse. The width and the area of the pulse are indicative of particle transit time and hence strongly influenced by the flow speed of sample analysis and the size of the cell being detected (27), while the peak of the signal is expected to reflect the total fluorescence of the cell and therefore it was the parameter chosen to estimate the intra-cellular Chl-a content.

### Field sampling

Field data consisted of 20 samples taken from 12<sup>th</sup> to 14<sup>th</sup> April of 2013 in coastal, shelf and oceanic waters of the Cantabrian Sea (Southern Bay of Biscay) (43.51-43.80°N, 5.55-3.73°W, 25-1625 m bathymetry). Sea-water samples were collected at selected depths

180

181

182

183

186

187

188

189

190

191

192

193

194

195

196

197

198

199

200

201

(ranging from 3 to 100 meters) with Niskin bottles mounted on a rosette sampler system equipped with a CTD (conductivity-temperature-depth) probe (SBE911), and auxiliary sensor for the measurement of underwater PAR (Biospherical/Licor radiometer). Surface PAR on an hourly basis was recorded on a meteorological station sited on land near the sampling area (43.54°N, 5.62°W, at 30 meters above mean sea level).

184 From the in situ PAR profile, the attenuation coefficient (kd) was estimated with the 185 light extinction equation,

$$I_z = I_0 \times e^{(-z \times k_d)}$$
 Eq. 1

where I<sub>z</sub> and I<sub>0</sub> represent, respectively, irradiance at a given depth and in the surface, and z is the depth in the water column. To integrate the irradiance regime experienced by the cells of a given sample the field irradiance at the sample depth was estimated taking into account the 24 hours PAR regime previous to the time of acquisition of the sample (only light hours), calculated from surface solar radiation and assuming a constant k<sub>d</sub>, and weighting the calculated underwater PAR by the elapsed time. Field irradiances ranged from 1 to 1604 µmol photons m<sup>-2</sup> s<sup>-1</sup>.

Downloaded from http://aem.asm.org/ on February 9, 2017 by UNIV OF CALIF SAN DIEGO

Phytoplankton samples were analyzed on board with FlowCAM. They were maintained fresh and in the dark until analysis, which started immediately after collection to minimize pigment degradation. Each sample was split in two: an un-concentrated subsample pre-filtered by 40 μm for analysis with 200× magnification and 50 μm flow chamber (1 mL), and a concentrated subsample pre-filtered by 100 µm (1 liter down to around 20 mL) for analysis with 100× magnification and 100 µm flow chamber (10 mL). The sample concentration was carried out by reverse filtration (28) through a 15 µm mesh to prevent the damage of living cells. A detailed description of the protocol for FlowCAM sample analysis can be consulted elsewhere (29).

### Data analysis

202

203

204

205

206

207

208

209

210

211

212

213

214

215

216

217

218

For each sample, either cultured or natural, abundance of autotrophic cells was estimated from all cells imaged by the FlowCAM in the fluorescence-triggered mode. The size of the cells was estimated considering only properly focused and uncut single cells. The spherical equivalent diameter (ESD) and geometrical section of each cell were obtained directly from the digital image taken by the FlowCAM, and particle biovolume was calculated as a revolution volume from the ESD of the particles. Fluorescence signals were selected considering only uncut cells captured in the proximities of the laser beam. FlowCAM photographs with more than one particle were rejected.

Experiments 1 to 4 were used to explore the variability of fluorescence measurements, in parallel lines of the incubator (experiments 1-4) and in replicate analysis of the same sample (experiment 1). Experiments 5 to 12 were used to obtain a fluorescence to Chl-a conversion and to explore the inter- and intra-specific scaling of chlorophyll content. We categorized the day of sample extraction according to the growth phase of the culture, as being in exponential phase or not, by plotting the evolution of carbon biomass. From the initial carbon content (C<sub>0</sub> at time t<sub>0</sub>) to the content in the last day of sample extraction (C<sub>t</sub> at time t) we estimated the specific growth rate ( $\mu$ ):

Downloaded from http://aem.asm.org/ on February 9, 2017 by UNIV OF CALIF SAN DIEGO

$$C_t = C_0 \times e^{\mu(t-t_0)}$$
 Eq. 2

and the number of generations (g) experienced by the population from the initial sample. 219

$$g = log_2(C_t/C_0)$$
 Eq. 3

220 To check whether the photoacclimation has being completed at the end of the incubations, we 221 compared the carbon and chlorophyll cell content between the mid-term and last sample day 222 of experiments 8 and 11 (days 4 and 6).

# Results

223

224

225

226

227

228

229

230

231

232

233

234

235

236

237

238

239

240

241

242

243

244

245

### Variability of the fluorescence signal

Experiments 1 to 4 took place each in two parallel incubator lines, being the treatments analyzed by duplicate (line replicate). Additionally, in experiment 1 samples of the first line were analyzed by duplicate (aliquot replicate). These results were used to account for the variability of the fluorescence signal detected by FlowCAM. Fluorescent beads analyzed each sampling day (between 64 and 768 items) presented average values of 181 ± 14 fluorescence units with the 20x lens and of  $41 \pm 19$  units with the 10x lens. The variability between average values in parallel incubations (Fig. 1A) was ±38 units of fluorescence per cell (95% c.i.), whereas the variability between aliquots of the same incubation line (Fig. 1B) was of ±4 units of fluorescence per cell. The standard deviation within each FlowCAM run was in all cases higher than differences in average values between experimental (line or aliquot) replicates. This indicates that the fluorescence signal was constant enough to compare different experiments or treatments (inter-specific variation) and sensitive enough to distinguish differences among cells of the same population (intra-specific variation).

Downloaded from http://aem.asm.org/ on February 9, 2017 by UNIV OF CALIF SAN DIEGO

### Phytoplankton incubations

Experiments 5 to 12 were used to obtain a fluorescence to Chl-a conversion and to explore the inter- and intra-specific scaling of chlorophyll content. Although the number of generations experienced in each experiment since the beginning to the last day was variable (Table II), the experiments sampled also in the mid-term (8 and 11) twice confirmed that the relative composition of the cells kept constant for most of the light treatments from the the mid-term sample to that at the end of the incubation, indicating that the cells were already acclimated to culture conditions (Fig. 2).

247

248

249

250

251

252

253

254

255

256

257

258

259

260

261

262

263

264

265

266

267

268

269

The average fluorescence per unit volume and the average intracellular Chl-a concentration in the last day of incubation varied as a function of growth irradiance (Fig. 3) in all experiments. The pigment concentration obtained through Chl-a extraction decreased as expected with increased irradiance and the same pattern was captured by the FlowCAMmeasured fluorescence: fluorescence intensity decreased with irradiance in parallel to intracellular pigment content. The only exception was experiment 11, which showed higher fluorescence at intermediate growth irradiances, but maintaining the general decreasing pattern for higher values.

### Fluorescence to Chl-a conversion

To explore the relationship between the fluorescence measured by the FlowCAM and the Chl-a content, we analyzed the relationship between the average (peak) fluorescence per cell (arbitrary units cell-1) and the average intracellular pigment content per cell (pg Chl-a cell-1) in the last day of the incubation experiments (Fig. 4). Since the fluorescence signals measured with different combinations of FlowCAM magnification lenses / flow chamber dimensions (FC) were not comparable due to optical differences, the relationship was explored for each of the applied combinations (200x/FC50 and 100x/FC100).

Downloaded from http://aem.asm.org/ on February 9, 2017 by UNIV OF CALIF SAN DIEGO

A priori, a linear relation would be expected between fluorescence and the absorption cross section of single cells (30), which implies a nonlinear relationship with the Chl-a content given the package effect. The package effect entails that larger cells can expose relatively less pigments for light harvesting than smaller cells due to constraints imposed by the relationship between cell surface area and volume (3, 4, 31). The best fit (lowest Akaike score) between fluorescence and Chl-a per cell was given by a curvilinear model. We performed a linear regression over the log-log transformed data to adjust an exponential curve to the experimental data obtained with the 200×/FC50 (F = 75.46 × Chl- $a^{0.4}$ , R<sup>2</sup> = 0.85, p-

273

274

275

276

277

278

279

280

281

282

283

284

285

286

287

288

289

290

291

292

value<0.001, Fig. 4A) and the  $100 \times /FC100$  (F =  $40.63 \times Chl-a^{0.28}$ , R<sup>2</sup> = 0.91, p-value<0.001, 270 271 Fig. 4B).

### Inter-specific scaling of chlorophyll content

For each irradiance level, we combined the data for the different species and explored the relationship between Chl-a content and cell biovolume. Figure 5 shows both the analytical Chl-a estimates (upper panels) and the estimates derived from FlowCAM's fluorescence using the fluorescence to Chl-a conversions described above (lower panels), as a function of body size for the different irradiance treatments. A reduced major axis regression on the logtransformed data was used to estimate the allometric size-scaling exponent at each irradiance level (Fig. 5). The size-scaling exponents were estimated additionally (dashed lines) only with experiments that kept growing in exponential phase as indicated in Table II. The size-scaling exponents of Chl-a content increased with irradiance from 0.65 to 0.83 (Fig. 5A-E) which translates in the decrease of the size scaling exponent with increasing light limitation (Fig. 6A). Similarly, the pattern of decrease of the size scaling exponent in light limited conditions was captured by the FlowCAM-measured fluorescence (Fig. 6B). Considering this Chl-a predicted from fluorescence, the exponents of the size dependence of pigment content at each irradiance level were slightly higher, varying between 0.77 and 0.90 (Fig. 5F-J).

Downloaded from http://aem.asm.org/ on February 9, 2017 by UNIV OF CALIF SAN DIEGO

### Intra-specific scaling of chlorophyll content

The measurement of fluorescence on a single-cell basis allowed us to explore the size dependence of Chl-a content within single populations. To analyze the size dependence of Chl-a content as a function of irradiance within each treatment, the fluorescence of each single cell was converted to Chl-a content and plotted against cellular biovolume in a log-log scale. As an example, the five irradiance treatments in experiment 9 (K. micrum) appear in

294

295

296

297

298

299

300

301

302

303

304

305

306

307

308

309

310

311

312

313

314

315

316

Figure 7 (increasing irradiance from panel A to E). The distributions of biovolume and Chl-a per cell were log-normal, as indicated by the bar plots in the x and y axis. The dispersion of the data and the presence of outliers are more evident at high irradiance levels. The size scaling exponent was obtained using robust linear regression, an alternative to least squares regression less sensitive to outliers (32), and tested for statistical significance.

Considering a single species, the size scaling exponent tended to decrease in light limited conditions, similarly to what happens at the inter-specific level. Figure 8 shows the variation of the size-scaling exponents that resulted significant (p-value<0.05) as a function of irradiance for each of the eight experiments. To visualize the trend, we adjusted linear and logarithmic models to the data and plotted the 95% confidence interval of the model with the lowest Akaike score. All experiments except 5 and 10 showed a pattern of increase of the size-scaling exponent at increased growth irradiance levels. Experiment 5 did not show this pattern, probably due to the small size of I. galbana, very close to the detection limit of the FlowCAM.

Downloaded from http://aem.asm.org/ on February 9, 2017 by UNIV OF CALIF SAN DIEGO

The intra-specific scaling exponents were not limited to 1, as found at the inter-specific scale, but fluctuated between 0.35 and 3.04 with variability within each experiment ranging between 0.1 and 1.52 units. Despite the reduced biovolume range within a single species, the relationship with body size was significant in most cases (in 41 of 42 light treatments, pvalue<0.05) and body size explained between 3 and 28% of the variability in the Chl-a content.

### Field sampling

The size scaling of Chl-a content was reproduced in the natural samples analyzed. The fluorescence values in the two subsamples analyzed for each sample were converted to Chl-a content and combined to estimate a size scaling exponent for each sample. The exponents of

318

319

320

321

322

323

324

325

Downloaded from http://aem.asm.org/ on February 9, 2017 by UNIV OF CALIF SAN DIEGO

the size dependence were estimated by robust linear regression and test for significance (pvalue<0.05). Figure 9A shows an example of a natural sample, with cells imaged with the 200×/FC50 (light dots) and with the 100×/F100 (dark dots), and the linear fit. Among all samples, the size scaling exponent ranged from 0.5 to 1 (Fig. 9B) and body size explained between 27 to 59% of the variability in the predicted Chl-a content. In natural samples, the influence of other environmental variables, such as temperature and nutrient concentrations, and the physiological (ontogenetic) status of the cells (exponential growth, stationary or senescence phases) resulted in a poor correlation between the size-scaling exponent and field irradiance.

# Downloaded from http://aem.asm.org/ on February 9, 2017 by UNIV OF CALIF SAN DIEGO

### Discussion

326

327

328

329

330

331

332

333

334

335

336

337

338

339

340

341

342

343

344

345

346

347

348

349

350

The existence of a relationship between the fluorescence measured by flow cytometers and the Chl-a per cell has been described before (24) but, for the best of our knowledge, this is the first time that this relationship is explored using FlowCAM and extended to microphytoplankton. The intracellular concentration of Chl-a has been estimated for the whole phytoplankton community or for specific compartments (33, 34), but we have shown that the simultaneous acquisition of estimates of cell size, cell abundance and fluorescence per cell by means of FlowCAM offers an integrated methodology to estimate intracellular concentration of Chl-a of nano- and micro-phytoplankton on an individual, single cell basis, allowing the characterization of the size dependence of Chl-a content in natural samples.

Although useful as a proxy for Chl-a content, there are limitations when estimating Chla from fluorescence, given the presence of other energy dissipating processes and also the variability of the fluorescence quantum yield itself. There are diverse processes competing with fluorescence to de-excite the molecule of Chl-a, such as internal conversion, resonance energy transfer, quenching and bleaching (35, 36), that may change the energy exchange rate, making the fluorescence signal no longer proportional to the amount of pigment. Through photochemical quenching, the liberation rate of electrons from photosystems increases due to enzymatic activity, and through non-photochemical quenching the heat dissipation is increased. Whereas photochemical quenching can be relevant in solar-stimulated Chl-a fluorescence, it is negligible in the laser-stimulated fluorescence, provided the flash is of high intensity and short length (37). It is not possible to inhibit heat dissipation totally but it can be minimized if the measurements are taken on dark adapted, non-stressed cells (38).

On the other hand, the quantum yield for chlorophyll fluorescence is not constant across species, neither across physiological conditions. There are variations in the emission of fluorescence of Chl-a under constant light conditions, which can indicate a vital cycle in Chl-

352

353

354

355

356

357

358

359

360

361

362

363

364

365

366

367

368

369

370

371

372

373

374

Downloaded from http://aem.asm.org/ on February 9, 2017 by UNIV OF CALIF SAN DIEGO

a synthesis (39). When performing a calibration, this problem is common to all fluorimetric methods for chlorophyll estimation, and reference values already account for variations in quantum yield. In our experiments, spectrofluorimetry-determined Chl-a and FlowCAMdetermined fluorescence suffered the same bias and hence, we considered both approaches comparable. A different scenario occurs when the fluorescence measurement is applied to new samples without reference values. Since different environmental conditions, such as nutrient availability or temperature, may lead to widely different quantum yield of chlorophyll, it is a matter of debate common to all fluorometric methods that estimate chlorophyll from in situ fluorescence to what extent a calibration made with a limited set of samples can be extrapolated to other samples acquired for a different range of environmental conditions.

Beyond overall limitations, we consider that the extrapolation to natural samples of the fluorescence to Chl-a conversion we have obtained is reasonably because our relationship has been estimated combining different species and different growth conditions. Previous correlations between fluorescence and Chl-a in single cells (24) were species specific, which prevented its use it in a routine basis for the estimation of Chl-a content for the whole phytoplankton community. We found a curvilinear correlation between fluorescence and Chla content that resulted taxon independent and, if not independent of growth status, at least it encompassed the variability in pigment content due to growth rate.

### Inter-specific size dependence of chlorophyll content

A taxon independent conversion allowed us to estimate the Chl-a content in different cultures covering an ample size range, and hence, enabling the analysis of the size scaling of chlorophyll content. Larger cells tend to have lower cellular pigment concentrations than smaller cells under similar environmental conditions (40), to counteract the package effect

376

377

378

379

380

381

382

383

384

385

386

387

388

389

390

391

392

393

394

395

396

397

398

associated with increasing cell size (15). This means that Chl-a content per cell scales with size with exponents lower than one, which is supported by geometrical considerations (3, 4). This theoretical predictions were supported by empirical data (16, 20) and consistent with our results based on fluorescence-based Chl-a estimates.

As growth irradiance decreased, the exponent of the size-scaling of Chl-a content decreased, as described by previous empirical works (20). All cells incremented their pigment content but, relative to body size, the increment of pigment was larger in small cells than in larger cells. Theoretical models have predicted an upper limit for the exponent of 3/4 under saturating irradiance (15), but our exponents surpass this predicted value.

We are aware, however, that the results derived from the inter-specific analyses need to be taken with caution for two reasons. The first one is that in order to get cells of different sizes it was necessary to combine different species. Changes in light harvesting characteristics that are correlated with cell size can alter the size scaling of chlorophyll content. For example, a systematic shift in cell shape can reduce the package effect and mitigate the potential reduction in the size-scaling exponent of cellular pigment concentration and growth rates (15). The second caveat is that the growth status of the combined cultures must be the same, e.g. exponential growth. When estimating the exponent of the size-scaling of Chl-a content only with cultures in exponential growth, the number of data are reduced and the exponents differed from previous described (Fig. 6A). So the relevance of the size scaling exponents obtained combining all cultures could be obscured by the fact that not all populations where in the same growth phase.

It is crucial to compare organisms with similar pigment composition under similar growth conditions when calculating and comparing the size-scaling exponent of cellular pigment concentration. The estimation of the allometric exponents on single populations

400

401

402

403

404

405

406

407

408

409

410

411

412

413

414

415

416

417

418

419

420

421

422

(thanks to the single cell approach) avoids the interspecific variability, but also covers a size range where all cells are in the same growth regime.

### Intra-specific size dependence of chlorophyll content

At the intra-specific scale, the variability of fluorescence values, and hence Chl-a content, was higher than that for size. Size only explained a comparatively small part of the variability of intracellular Chl-a content because of the narrow biovolume range covered, but also due to phenotypic (and to some extent also genotypic) variability among the individuals of the population and differences in the phase of the cellular cycle and physiological status. Nevertheless, the same pattern of decrease of the size scaling exponent of Chl-a content per cell in light limited conditions was found when focusing on a single species, which means that, for a generalized increment in pigment content in light limited conditions, the smaller cells had a larger margin for pigment accumulation.

Downloaded from http://aem.asm.org/ on February 9, 2017 by UNIV OF CALIF SAN DIEGO

This is the first time this fact is observed in single populations and it means that not only smaller species maintain higher photosynthetic rates under light limitation (41) but also smaller cells within the same population. The optical absorption cross section of pigments and the intra-cellular concentration of components that capture photon energy are physiological traits that underlie growth/production traits (42). Consequently, different cell sizes limited in the range of their plasticity for pigment content results in intra-specific differences in the integrated growth response to irradiance. Thus, the variation in the size scaling of Chl-a content also predicts shifts in the size scaling of growth and photosynthesis with the light regime. All phytoplankton require light for growth and the variable light regimes experienced by the cells and imposed by water column mixing may explain the size-structure of the phytoplankton community (43, 44). As a result, the differences in pigment content as a function of cell size lead to different physiological strategies and niche partitioning.

424

425

426

427

428

429

430

431

432

433

434

435

436

437

438

439

440

441

442

443

444

445

446

447

We have found that the size-scaling of Chl-a content per cell of a single population has exponents higher than one for some species, which means that larger cells have higher Chl-a content per unit volume than smaller cells. This result can be counter-intuitive. It may be explained, however, if the difference in cell size and pigment content within the population is due, to great extent, to the phase of the cellular cycle experienced by the cells. In unicellular phytoplankton, within a given population, small cells are generated from larger cells, so, cell division may be important reducing the package effect for young daughter cells (39). A large cell with a given Chl-a concentration that enters the division phase of the cellular cycle will give place to two smaller cells with half the Chl-a content, which is lower than the potential concentration that their new surface-to-volume ratio may allow. In this case, the concentration of Chl-a will be independent of cell size and the pigment content per cell will scale with size with an exponent around one. On the other extreme, a large cell can increase its pigment content above the limits imposed by its surface-to-volume ratio in order to divide this pigment between the two daughter cells, as it happens in coccolithophorids (45).

For the smallest species, other biovolume constrains can be considered. Very small cells might be prevented from increasing their scalable components (photosynthetic units) due to the necessity of maintaining a constant quota of non-scalable essential components, such as the gene pool, within a very small cell biovolume (46). In this case, only those cells above a critical size will be able to increase their intracellular quota of molecules involved in metabolic processes.

Downloaded from http://aem.asm.org/ on February 9, 2017 by UNIV OF CALIF SAN DIEGO

Another source of uncertainty is the one related with the variability in the cellular content of other pigments. Phytoplankton cells might be able to respond to changing light levels through the production of other pigments, such as accessory light-harvesting pigments or photo-protective pigments (47). The single-cell fluorescence method accounted for the specific fluorescent signature of a given pigment, which permitted to distinguish the patterns

449

450

451

452

453

454

455

456

457

458

459

460

461

462

463

464

465

466

467

468

469

470

471

472

found for different pigments (see Supplementary material for an analysis of phycoerythrin content in R. salina experiments). The pattern in the size dependence of the content in a photo-protective pigment is expected to follow the opposite pattern of a light-harvesting pigment, increasing the intracellular concentration and decreasing the size scaling exponent at light saturated conditions.

### In situ size dependence of chlorophyll content

Our approach, the analysis of single cells, is the unique choice to apply the same methodology to field samples and explore the size dependence of Chl-a content in situ under different environmental conditions. It also opens the door to the estimation of size-scaling per functional or taxonomic group. In this work, the natural samples yielded exponents lower than 1, in agreement with the results of the inter-specific size-scaling. However, a question that remained unsolved is whether the upper limit of the exponent is more likely to be 1 (17) or <sup>3</sup>/<sub>4</sub> (15). To the best of our knowledge, we reported for the first time the size scaling of Chl-a content in single cells, and our results showed maximum exponents lower than 1 but higher than 3/4, both in natural samples and cultures. An isometric scaling between cell volume and intracellular Chl-a has been reported on the basis of size-fractionation of Chl-a in natural samples by (17), who argued that the discrepancies between the exponents obtained in natural and in laboratory conditions could be due to the different growth conditions experienced by cultured cells and the small number of species used in laboratory studies.

Downloaded from http://aem.asm.org/ on February 9, 2017 by UNIV OF CALIF SAN DIEGO

The variability found on the intra-specific size-scaling of Chl-a content appeared also in natural samples, since different populations of the phytoplankton community present different physiologies and phases of their respective life cycles. The variation of the size scaling exponent as a function of irradiance was obscured in the field sampling, probably because the measured Chl-a content depends also on many other factors (e.g. the nutritional status of the cells) (6). Also, we have cultured only spherical or elliptical cells, but, in natural

474

475

476

477

478

479

480

481

482

483

484

485

486

487

488

489

490

491

492

493

494

495

496

communities, cells have developed strategies to escape from geometrical constrains on pigment content, such as the non-spherical shapes of diatoms and the presence of vacuoles (48).

The analysis of natural samples covers a wide range of environmental scenarios, from light or nutrient limitation to saturating conditions, which can help to understand how resource acquisition affect the productivity of natural communities. The size dependence of Chl-a content relates directly with the size scaling of photosynthetic rates. This can be determinant in primary productivity models since phytoplankton production can be modelled on a more realistic way improving current estimates derived from global primary production models. State of the art net primary production (NPP) models use carbon biomass instead of Chl-a concentration, since variability in intracellular Chl-a content from light acclimation and nutrient stress confounds the relationship between Chl-a and phytoplankton biomass (49, 50). In situ datasets as those obtained with FlowCAM, including cell size and Chl-a content, can be useful in the validation of these models.

Downloaded from http://aem.asm.org/ on February 9, 2017 by UNIV OF CALIF SAN DIEGO

### Acknowledgements

We are indebted to the Red Tides and Harmful Algae team of the Centro Oceanográfico de Vigo (IEO) for the supply of the clones of their Toxic Phytoplankton Culture Collection. We thank the captain and crew in the B/O Ángeles Alvariño for their assistance during the RADCAN 0413 cruise. F. Ronzón kindly provided solar radiation data from his meteorological station in Gijón. This work was supported by Fundación para el Fomento en Asturias de la Investigación Científica Aplicada y la Tecnología (FICYT) [research grant BP07-081 to E.A.], Ministerio de Economía y Competitividad (MINECO) [projects CTM2006-04854-MAR and CTM2009-13882-MAR to EN and ALU] and Instituto Español de Oceanografía (IEO) [project RADIALES].

### 497 References

- Cullen JJ. 1982. The deep chlorophyll maximum: comparing vertical profiles of 498 1. 499 chlorophyll a. Can J Fish Aquat Sci 39:791-803.
- 500 2. MacIntyre HL, Kana TM, Anning J, Geider RJ, Anning T, Geider RJ. 2002. 501 Photoacclimation of photosynthesis irradiance response curves and photosynthetic 502 pigments in microalgae and cyanobacteria. J Phycol 38:17-38.
- 503 Kirk JTO. 1975. A theoretical analysis of the contribution of algal cells to the 3. 504 attenuation of light within natural waters II.Spherical cells. New Phytol 75:21-36.
- 505 4. Kirk JTO. 1975. A theoretical analysis of the contribution of algal cells to the 506 attenuation of light within natural waters I.General treatment of suspensions of 507 pigmented cells. New Phytol 75:11-20.
- 508 Huot Y, Babin M, Bruyant F, Grob C, Twardowski MS, Claustre H. 2007. Does 5. 509 chlorophyll a provide the best index of phytoplankton biomass for primary productivity studies? Biogeosciences Discuss 4:707–745. 510
- 511 6. Geider RJ. 1987. Light and temperature dependence of the carbon to chlorophyll a 512 ratio in microalgae and cyanobacteria. New Phytol 34:1064.
- 513 7. Geider RJ, MacIntyre HL, Kana TM. 1998. A dynamic regulatory model of 514 phytoplanktonic acclimation to light, nutrients, and temperature. Limnol Ocean 515 **43**:679-694.
- 516 Tang EPY. 1996. Why do dinoflagellates have lower growth rates. J Phycol 32:80–84. 8.
- 517 9. Riemann B, Simonsen P, Stensgaard L. 1989. The carbon and chlorophyll content of 518 phytoplankton from various nutrient regimes. J Plankt Res 11:1037–1045.
- 519 10. Cullen JJ, Yang X, MacIntyre HL. 1992. Nutrient limitation of marine 520 photosynthesis, p. 70–88. In Falkowski, PG, Woodhead, AD (eds.), Primary 521 Productivity and Biogeochemical Cycles in the Sea. Springer, New York.
- 522 11. Yacobi YZ, Zohary T. 2010. Carbon: Chlorophyll a ratio, assimilation numbers and 523 turnover times of Lake Kinneret phytoplankton. Hydrobiologia 639:185–196.
- 524 12. Geider RJ, Platt T, Raven JA. 1986. Size dependence of growth and photosynthesis 525 in diatoms: a synthesis. Mar Ecol Prog Ser **30**:93–104.
- 526 13. Finkel Z V. 2001. Light absorption and size-scaling of light-limited metabolism in 527 marine diatoms. Limnol Ocean 46:86-94.
- 528 14. Mei ZP, Finkel Z V, Irwin AJ. 2009. Light and nutrient availability affect the size-529 scaling of growth in phytoplankton. J Theor Biol 259:582–588.
- Finkel Z V. 2004. Resource limitation alters the 3/4 size scaling of metabolic rates in 530 15. 531 phytoplankton. Mar Ecol Prog Ser 273:269–279.
- 532 Key T, McCarthy A, Campbell DA, Six C, Roy S, Finkel Z V. 2010. Cell size trade-16. 533 offs govern light exploitation strategies in marine phytoplankton. Env Microbiol 534 12:95-104.
- 535 Marañón E, Cermeño P, Rodríguez J, Zubkov M V, Harris RP. 2007. Scaling of 536 phytoplankton photosynthesis and cell size in the ocean. Limnol Ocean 52:2190–2198.
- 537 Pérez V, Fernández E, Marañón E, Morán XAG, Zubkov M V. 2006. Vertical 18.

- 538 distribution of phytoplankton biomass, production and growth in the Atlantic 539 subtropical gyres. Deep Res I 53:1616–1634.
- 540 19. Harrison PJ, Conway HL, Holmes CR, Davis CO. 1990. Effects of nutrients and 541 light on the biochemical composition of phytoplankton. J Appl Phycol 2:45–56.
- 542 20. Fujiki T, Taguchi S. 2002. Variability in chlorophyll a specific absorption coefficient 543 in marine phytoplankton as a function of cell size and irradiance. J Plankt Res 24:859-544
- 545 Yentsch CM, Horan PK, Muirhead K, Dortch O, Hangen F, Legendre L, Murphy 21. 546 LS, Perry MJ, Phinney DA, Pomponi SA, Spinrad RW, Wood M, Yentsch CS, 547 Zahuranec BJ. 1983. Flow cytometry and cell sorting: a technique for analysis and 548 sorting of aquatic particles. Limnol Ocean 28:1275–1280.
- 549 Lorenzen CJ. 1966. A method for the continuous measurement of in vivo chlorophyll 22. 550 concentration. Deep Res 13:223-227.
- 551 Yentsch CS, Menzel DW. 1963. A method for the determination of phytoplankton 23. 552 chlorophyll and phaeophytin by fluorescence. Deep Res 10:221–231.
- Sosik HM, Chisholm SW, Olson RJ. 1989. Chlorophyll fluorescence from single 553 24. 554 cells: interpretation of flow cytometric signals. Limnol Ocean 34:1749–1761.
- 555 Sieracki CK, Sieracki ME, Yentsch CS. 1998. An imaging-in-flow system for 25. 556 automated analysis of marine microplankton. Mar Ecol Prog Ser 168:285–296.
- 557 26. Steinberg MK, First MR, Lemieux EJ, Drake LA, Nelson BN, Kulis DM, Anderson DM, Welschmeyer NA, Herring PR. 2012. Comparison of techniques 558 559 used to count single-celled viable phytoplankton. J Appl Phycol 24:751–758.
- 560 27. Shapiro HM. 1941. Practical flow cytometry4th editio. Book, Wiley-Liss, Hoboken, 561 New Jersey.
- 562 28. Dodson AN, Thomas WH. 1978. Reverse filtration, p. 104–107. In A., S (ed.), Phytoplankton manual. Book Section, UNESCO, Paris. 563
- 564 29. Álvarez E, Moyano M, López-Urrutia Á, Nogueira E, Scharek R. 2014. Routine 565 determination of plankton community composition and size structure: A comparison 566 between FlowCAM and light microscopy. J Plankton Res **36**:170–184.
- Perry MJ, Porter SM. 1989. Determination of the cross-section absorption coefficient 567 30. 568 of individual phytoplankton cells by analytical flow cytometry. Limnol Ocean 569 **34**:1727–1738.
- 570 31. Morel A, Bricaud A. 1986. Inherent optical properties of algal cells including phytoplankton: theoretical and experimental results, p. 521-559. In Platt, T, Li, WKW 571 572 (eds.), Photosynthetic picoplankton. Book Section, Can. Bull. Fish. Aquat. Sci.
- 573 Venables WN, Ripley BD. 2002. Modern applied statistics with S, 4th ed. Book, 32. 574 Springer, New York.
- 575 Sathyendranath S, Stuart V, Nair A, Oka K, Nakane T, Bouman H, Forget M-H, 33. 576 Maass H, Platt T. 2009. Carbon-to-chlorophyll ratio and growth rate of phytoplankton 577 in the sea. Mar Ecol Prog Ser 383:73-84.
- Wang XJ, Behrenfeld MJ, Le Borgne R, Murtugudde R, Boss E. 2009. Regulation 578 34. 579 of phytoplankton carbon to chlorophyll ratio by light, nutrients and temperature in the 580 equatorial Pacific Ocean: a basin-scale model. Biogeosciences Discuss 5:3869–3903.

- 581 Falkowski PG, Kiefer D a. 1985. Chlorophyll a fluorescence in phytopankton: 582 relationship to photosynthesis and biomass. J Plankt Res 7:715–731.
- 583 36. Sakshaug E, Bricaud A, Dandonneau Y, Falkowski PG, Kiefer DA, Legendre L, 584 Morel A, Parslow J, Takahashi M. 1998. Parameters of Photosynthesis: Definitions, 585 Theory and Interpretation of Results. J Plank Res 19:1637–1670.
- 586 Bradbury M, Baker NR. 1981. Analysis of the slow phases of the in vivo chlorophyll fluorescence induction curve. Changes in the redox state of Photosystem II electron 587 588 acceptors and fluorescence emission from Photosystems I and II. Biochim Biophys 589 Acta - Bioenerg **635**:542–551.
- 590 Maxwell K, Johnson GN. 2000. Chlorophyll fluorescence - a practical guide. J Exp 38. 591 Bot 51:659-668.
- 592 39. Baird ME, Ralph PJ, Rizwi F, Wild-allen K, Steven ADL. 2013. A dynamic model 593 of the cellular carbon to chlorophyll ratio applied to a batch culture and a continental 594 shelf ecosystem. Limnol Ocean 58:1215-1226.
- 595 40. Agustí S. 1991. Allometric scaling of light absorption and scattering by phytoplankton cells. Can J Fish Aquat Sci 48:763-767. 596
- 597 41. Dubinsky Z, Stambler N. 2009. Photoacclimation processes in phytoplankton: 598 mechanisms, consequences, and applications. Aquat Microb Ecol 56:163-176.
- 599 42. Edwards KF, Thomas MK, Klausmeier CA, Litchman E. 2015. Light and growth in 600 marine phytoplankton: allometric, taxonomic, and environmental variation. Limnol Ocean 0:1-21. 601

Downloaded from http://aem.asm.org/ on February 9, 2017 by UNIV OF CALIF SAN DIEGO

- 602 Karentz D, Cleaver JE, Mitchell DL. 1991. Cell survival characteristics and 43. 603 molecular responses of Antarctic phytoplankton to ultraviolet-B radiation. J Phycol 604
- 605 44. Finkel Z V, Vaillancourt CJ, Irwin AJ, Reavie ED, Smol JP. 2009. Environmental 606 control of diatom community size structure varies across aquatic ecosystems. Proc R 607 Soc B **276**:1627–1634.
- 608 Klaveness D. 1972. Coccolithus huxleyi (Lohm.) Kamptn II. The flagellate cell, 45. 609 aberrant cell types, vegetative propagation and life cycles. Br Phycol J 7:309–318.
- 610 46. **Raven JA.** 1998. Small is beautiful: the picophytoplankton. Funct Ecol 12:503–513.
- 611 47. Lutz VA, Sathyendaranath S, Head EJH, Li WKW. 2001. Changes in the in vivo 612 absorption and fluorescence excitation spectra with growth irradiance in three species 613 of phytoplankton. J Plankt Res 23:555–569.
- Raven JA, Callow JA. 1997. The vacuole: a cost-benefit analysis, p. 59–82. In Leigh, 614 48. 615 RA, Sanders, D (eds.), The plant vacuole. Book Section, Academic Press, San Diego.
- 49. Behrenfeld MJ, Boss E, Siegel DA, Shea DM. 2005. Carbon-based ocean 616 617 productivity and phytoplankton physiology from space. Glob Biogeochem Cycles 19:GB1006. 618
- 619 Westberry T, Behrenfeld MJ, Siegel DA, Boss E. 2008. Carbon-based primary 620 productivity modeling with vertically resolved photoacclimation. Glob Biogeochem 621 Cycles 22:GB2024.

622 623

Applied and Environmental Microbiology

Table I. Incubation conditions. Description of growth conditions of the incubation experiments carried out to obtain a gradient of Chl-a content per cell in seven different phytoplankton species.

Experiment	Species	Number of light treatments	Photo- period	Total days	Days of measurements	Lens / flow chamber	Number of points for the calibration
1	Isochrisis	5	12/12	4	4	20x/FC50	=
2	Isochrisis	5	12/12	6	6	20x/FC50	-
3	Isochrisis	5	12/12	1	1	20x/FC50	-
4	Prorocentrum	2	12/12	1	1	20x/FC50	-
5	Isochrisis	5	12/12	6	1 and 6	20x/FC50	5
6	Emiliana	5	12/12	5	1 and 5	20x/FC50	5
7	Rhodomonas	5	12/12	6	1 and 6	20x/FC50	5
8	Rhodomonas	6	14/10	6	1, 4 and 6	20x/FC50	12
9	Karlodinium	5	12/12	6	1 and 6	20x/FC50	5
10	Alexandrium	5	12/12	6	1 and 6	10x/FC100	5
11	Alexandrium	6	14/10	6	1, 4 and 6	10x/FC100	12
12	Protoceratium	5	12/12	6	1 and 6	10x/FC100	5

Downloaded from http://aem.asm.org/ on February 9, 2017 by UNIV OF CALIF SAN DIEGO

627 628

624

625

626

630

631 632

633

634

635

Table II. Incubation results. Cell-size, cellular composition (carbon and analytical Chl-a), fluorescence peak, growth rate (µ) and number of generations experienced (g) during the six experiments (Exp. 5 to 12, Table I) gathered to estimate the conversion from fluorescence to intra-cellular Chl-a, and the allometry of Chl-a content. Note that for experiments 8 and 11, the composition and growth parameters have been estimated not only for the last day of the incubation but also for the mid-term sampling (i.e. day 4). The asterisks in  $\mu$  values indicate those cultures that kept growing in exponential phase.

Exp	Light [µmol photons m <sup>-2</sup> s <sup>-1</sup> ]	day	ESD [µm]	C [pg cell <sup>-1</sup> ]	Chl-a [pg cell <sup>-1</sup> ]	Fluorescence peak ± sd	μ [d <sup>-1</sup> ]	g
5	115	6	4.0	5.6	0.28	45 + 20	0.29*	2.5
5	230	6	4.4	7.1	0.18	41 + 19	0.45*	3.9
5	460	6	4.2	6.4	0.14	37 + 18	0.57*	5.0
5	920	6	4.5	7.3	0.15	30 + 17	0.54*	4.7
5	1839	6	4.7	8.4	0.10	27 + 14	0.57*	5.0
6	115	5	4.5	7.7	0.98	50 + 22	-0.50	-2.3
6	230	5	5.1	10.6	0.86	46 + 28	-0.45	-1.9
6	460	5	5.1	10.4	0.55	56 + 27	-0.43	-1.3
6	920	5	5.0	10.1	0.21	55 + 25	0.00	0.7
6	1839	5	4.4	7.1	0.20	40 + 21	0.37*	1.8
7	115	6	7.3	26.1	1.93	109 + 20	0.38*	3.6
7	230	6	7.8	30.5	2.05	108 + 20	0.66*	5.4
7	460	6	8.2	35.3	1.74	98 + 22	0.74*	6.3
7	920	6	7.8	31.0	1.35	85 + 23	0.91*	6.6
7 8	1839 55	6	7.8	30.9 34.1	0.47 2.40	87 + 25 $109 + 29$	0.35*	0.2
	92	-	8.1				0.03	
8	230	4 4	8.6 8.5	40.1 38.0	2.23 2.27	100 + 26 83 + 25	0.15	0.8
8 8	382	4	8.3 9.0	38.0 44.0	2.27	83 + 23 $100 + 27$	0.23 0.24	1.3 1.4
8	828	4	9.0 8.7	40.3	1.50	83 + 24	0.24	2.2
8	1563	4	8.6	39.1	1.46	80 + 26	0.39	1.0
8	55		8.4	37.4	3.42	$\frac{80+20}{105+26}$	-0.06	0.0
8	92	6	8.4	36.9	3.36	105 + 26 $105 + 27$	0.01	0.0
8	230	6	8.4	37.2	2.53	105 + 27 $105 + 25$	0.01	1.4
8	382	6	8.6	39.8	2.03	87 + 26	0.43*	2.7
8	828	6	8.4	36.5	1.86	88 + 25	0.45	2.9
8	1563	6	9.8	55.3	1.56	99 + 27	0.25*	1.8
9	115	6	10.1	60.5	4.42	168 + 25	0.46*	1.1
9	230	6	10.4	65.7	3.34	154 + 28	0.48*	2.5
9	460	6	10.3	64.9	2.48	133 + 27	0.51*	3.3
9	920	6	10.9	73.4	1.78	115 + 27	0.66*	3.5
9	1839	6	10.2	62.8	1.56	106 + 28	0.61*	3.6
10	115	6	31.2	2018.8	30.57	101 + 39	-0.16	-1.1
10	230	6	35.3	2889.5	31.34	98 + 36	-0.20	-1.1
10	460	6	33.9	2498.7	21.64	104 + 32	-0.18	-0.8
10	920	6	35.2	2836.9	15.51	102 + 29	-0.29	-1.3
10	1839	6	37.1	3286.7	9.89	94 + 27	-0.19	-1.1
11	37	4	23.7	888.2	10.99	73 + 24	-0.19	-1.1
11	69	4	23.4	867.3	7.96	76 + 24	-0.12	-0.7
11	152	4	22.3	754.8	7.42	71 + 26	-0.08	-0.5
11	276	4	21.4	677.8	4.55	65 + 25	0.05	0.3
11	598	4	21.9	720.3	3.66	60 + 26	0.07	0.4
_11	1563	4	21.5	684.3	2.53	49 + 23	0.10	0.6
11	37	6	23.5	884.6	8.07	60 + 24	0.04	-0.9
11	69	6	23.4	864.8	7.46	70 + 22	-0.10	-1.0
11	152	6	22.3	756.3	6.33	72 + 24	0.02	-0.4
11	276	6	21.2	654.6	4.94	62 + 26	-0.06	0.1
11	598	6	21.1	642.6	3.71	55 + 25	-0.16	-0.2
11	1563	6	20.8	616.6	2.47	51 + 25	-0.15	0.1
12	115	6	28.7	1621.7	239.82	136 + 31	-0.87	-5.6
12	230	6	30.2	1849.0	53.34	126 + 26	-0.20	-3.7
12	460	6	32.0	2162.3	50.71	119 + 29	0.04	0.4
12	920	6	32.3	2225.8	48.86	109 + 27	-0.19	-0.5
12	1839	6	32.4	2231.7	40.73	111 + 26	-0.10	-1.7

Downloaded from http://aem.asm.org/ on February 9, 2017 by UNIV OF CALIF SAN DIEGO

Figure legends

637

660

636

638	Figure 1. Variability (mean $\pm$ sd) of the fluorescence signal within (A) parallel lines of the
639	incubator during experiments 1 to 4 and (B) duplicate sample analysis during
640	experiment 1. Dashed lines indicate the 95% confidence interval.
641	Figure 2. Relative composition of the cells of (A) Rhodomonas sp. (exp. 8) and (B)
642	Alexandrium tamarense (exp. 11) in terms of the Chl-a to carbon ratio (mg g <sup>-1</sup> ) as a
643	function of incubation time in the different light treatments (graded from light to dark
644	grey corresponding from high to low irradiance levels).
645	Figure 3. Incubations overview. Fluorescence per biovolume unit (black dots) and
646	intracellular Chl-a concentration (white dots) as a function of growth irradiance
647	intensity ( $\mu$ mol photons m <sup>-2</sup> s <sup>-1</sup> ) in the last day of each experiment.
648	Figure 4. Fluorescence to Chl-a conversion. Fluorescence peak per cell measured by the
649	FlowCAM as a function of analytic Chl-a per cell, for the experiments analyzed with
650	the (A) 200×-FC50 and (B) 100×-FC100 lens-flow chamber combinations. Solid
651	line, equation and R <sup>2</sup> indicate the fitted conversion from fluorescence peak to Chl-a.
652	Figure 5. Inter-specific size scaling of Chl-a per cell. Size scaling obtained combining the
653	results from experiments 5 to 12 for each of the increasing (A to E) irradiance
654	treatments for analytical Chl-a (each experiment provided a unique Chl-a value,
655	hence vertical error bars are not available) and for the increasing (F to ${\bf J}$ ) irradiance
656	treatments for fluorescence-based $Chl-a$ (standard deviation shown in vertical bars).
657	Solid lines include all experiments and dashed line in the upper panels only cultures
658	in exponential growth (Table II).
659	Figure 6. Size-scaling exponent of Chl-a per cell as a function of growth irradiance, (A) for

Downloaded from http://aem.asm.org/ on February 9, 2017 by UNIV OF CALIF SAN DIEGO

analytical Chl-a and (B) for fluorescence-based Chl-a. Size scaling exponent was

662

663

664

665

666

667

668

669

670

671

672

673

674

675

676

677

678

679

680

681

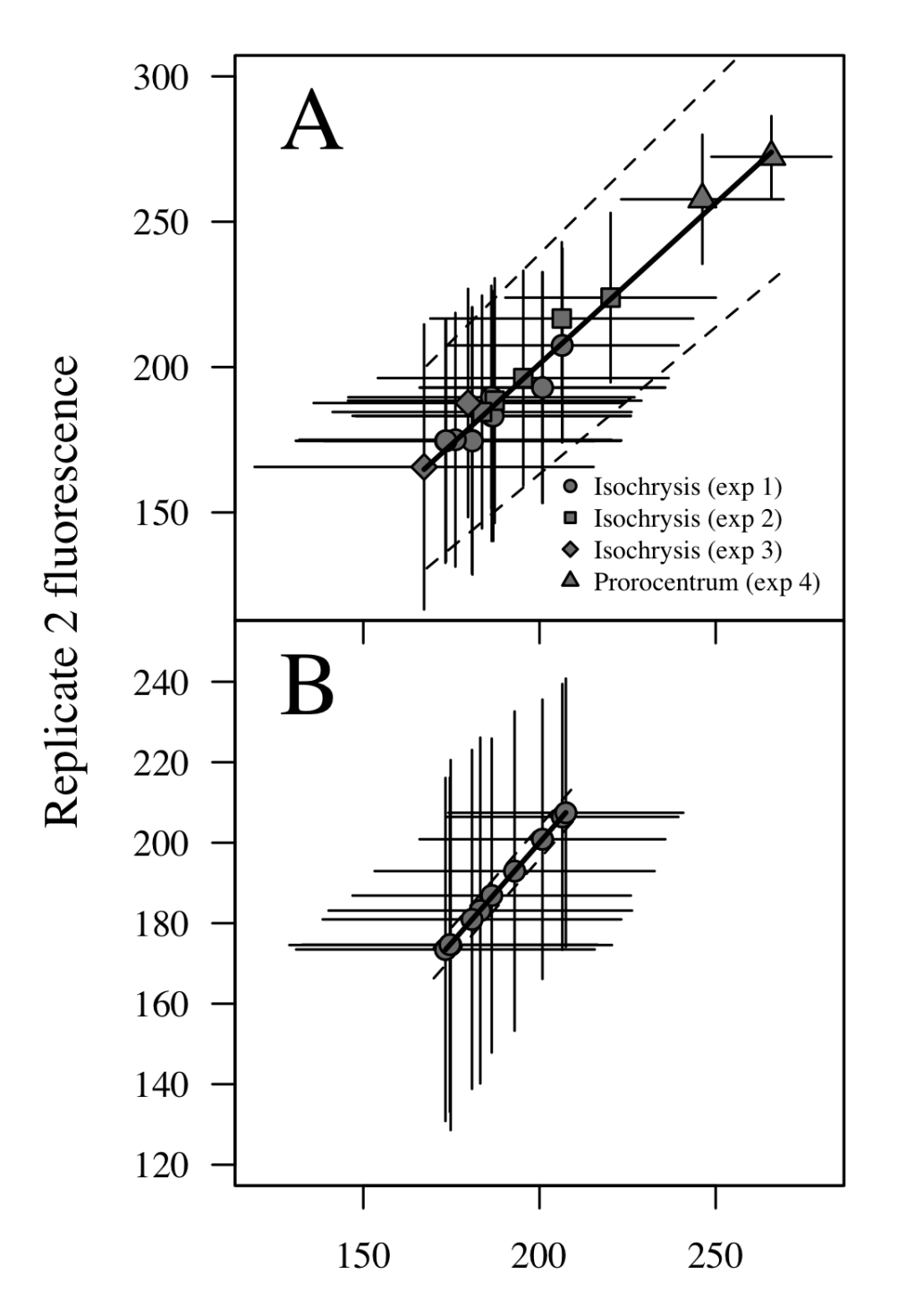
682

calculated from reduced major axis regression with standard deviation shown in vertical bars. Solid lines include all experiments and dashed line only cultures in exponential growth. Figure 7. Intra-specific size scaling of fluorescence-based Chl-a per cell. Population size scaling in the five increasing (A to E) irradiance treatments of experiment 9 (K. micrum). The size scaling exponent was obtained through robust linear regression, and the slope, R<sup>2</sup> of the relationship and the number of cells counted are shown in each panel. The asterisk in each panel indicates that the relationship was significant (p-value<0.05). Bar plots attached to the x and y axis show the distribution of cell biovolume and predicted Chl-a respectively. Figure 8. Change of the intra-specific size scaling with light. Intra-specific size scaling exponent for fluorescence-based Chl-a per cell as a function of growth irradiance for experiments 5 to 12 (Table II). The size scaling exponent was calculated from robust linear regression with standard deviation show in vertical bars. Solid lines indicate the confidence interval of the fitting with the lowest Akaike score, and the asterisk in each panel indicates that the relationship was significant (p-value<0.05).

Downloaded from http://aem.asm.org/ on February 9, 2017 by UNIV OF CALIF SAN DIEGO

Figure 9. Application to field sampling. (A) Example of the size scaling of fluorescencebased Chl-a per cell in a natural sample analyzed with the 200x (light dots) and the 100x magnification (dark dots). The size scaling exponent was obtained through robust linear regression, and the slope and R<sup>2</sup> of the fitting appear within the panel. (B) Size scaling exponent of fluorescence-based Chl-a per cell in a set of natural samples as a function of 24 hours field irradiance history.

683



Replicate 1 fluorescence

